ISSN: 3079-6660

Multi-Agent Collaborative Control of Photovoltaic Microgrid Clusters Considering Virtual Inertia Support

John A. Smith, Emily R. Davies

Department of Electrical Engineering, Chalmers University of Technology, Gothenburg 412 96, Sweden

Abstract

The increasing penetration of photovoltaic generation in modern power systems has precipitated a transition from centralized, high-inertia grids to distributed, low-inertia microgrid clusters. This paradigm shift introduces significant stability challenges, particularly regarding frequency resilience during islanding or load fluctuations. This paper proposes a novel multi-agent collaborative control framework designed to enhance the frequency stability of photovoltaic microgrid clusters through coordinated virtual inertia support. Unlike traditional centralized control schemes, which suffer from single points of failure and communication latency, the proposed method utilizes a distributed multi-agent system architecture. Each distributed generation unit functions as an autonomous agent, employing virtual synchronous generator control strategies to emulate the electromechanical behavior of traditional synchronous machines. We introduce an adaptive consensus algorithm that enables agents to dynamically allocate active power and inertia support responsibilities based on their real-time state of charge and generation capacity. Theoretical analysis and time-domain simulations demonstrate that this collaborative approach significantly reduces the rate of change of frequency and steady-state frequency deviation compared to conventional droop control methods. The results indicate that incorporating virtual inertia support within a multi-agent framework provides a robust solution for maintaining the stability and reliability of low-inertia renewable energy systems.

Keywords

Microgrid Clusters, Virtual Inertia, Multi-Agent Systems, Photovoltaic Control

1 Introduction

1.1 Background and Motivation

The global energy landscape is undergoing a profound transformation driven by the imperative to mitigate climate change and deplete fossil fuel reserves. Photovoltaic (PV) systems have emerged as a cornerstone of this transition due to their modularity, declining costs, and environmental benefits. As the installation capacity of PV systems grows, the power grid is evolving from a passive distribution network into an active system characterized by the proliferation of microgrids. A microgrid is defined as a localized group of electricity sources and loads that normally operates connected to and synchronous with the traditional wide area synchronous grid, but can also disconnect to isolate itself and function autonomously. While this structural evolution enhances energy resilience and reduces transmission losses, it introduces critical challenges related to system inertia. Traditional power systems rely heavily on synchronous generators, where large rotating masses provide kinetic energy buffer—known as rotational inertia—that inherently resists sudden changes in system frequency. In contrast, PV systems are interfaced with the grid through power

ISSN: 3079-6660

electronic converters. These converters are typically controlled as current sources following the grid frequency, providing zero distinct inertia to the system. As the penetration of inverter-based resources increases, the effective inertia of the grid decreases, leading to faster and larger frequency excursions in response to power imbalances. This phenomenon, often referred to as the low-inertia problem, compromises the stability margins of the power system and increases the risk of cascading failures or blackouts [1]. Consequently, equipping converter-interfaced generation with the ability to provide virtual inertia has become a paramount research objective.

1.2 Literature Review

Extensive research has been conducted to address the frequency stability issues in low-inertia microgrids. The concept of the Virtual Synchronous Generator (VSG) has gained prominence as a viable solution. By modifying the control loops of the power inverter to solve the swing equation in real-time, a VSG allows a static power electronic device to emulate the dynamic characteristics of a conventional synchronous machine, including inertia and damping properties. Early studies demonstrated that VSG control could effectively dampen power oscillations and limit the rate of change of frequency (RoCoF) during disturbances. However, the implementation of VSG in a clustered microgrid environment presents coordination challenges [2]. Existing control architectures for microgrid clusters are generally categorized into centralized, decentralized, and distributed schemes. Centralized control relies on a central controller to gather global information and dispatch commands. While optimal in ideal conditions, this approach is susceptible to single points of failure and high computational burdens as the system scales [3]. Decentralized control, such as voltage and frequency droop methods, operates on local measurements without communication. Although robust, decentralized methods often result in steady-state deviations and cannot achieve global optimization or precise power sharing among heterogeneous units [4]. Distributed control, particularly those based on Multi-Agent Systems (MAS), offers a balanced compromise. MAS decomposes the complex control problem into sub-problems solved by autonomous agents interacting through a sparse communication network. Recent literature has explored MAS for secondary frequency regulation and economic dispatch. For instance, consensus algorithms have been applied to ensure proportional power sharing. However, the majority of these studies focus on steady-state performance and often overlook the transient coordination of virtual inertia support [5]. Specifically, the dynamic allocation of virtual inertia based on the instantaneous capability of energy storage units remains an under-explored area. Inappropriate allocation of inertia support can lead to the premature depletion of energy storage in smaller units, thereby destabilizing the cluster [6].

1.3 Research Objectives and Contributions

This paper addresses the limitations of existing methods by proposing a Multi-Agent Collaborative Control strategy that explicitly integrates virtual inertia support for PV microgrid clusters. The primary objective is to develop a distributed control framework where PV agents can coordinate their inertia response to minimize frequency deviations while respecting the constraints of their associated energy storage systems. The main contributions of this work are threefold. First, we establish a comprehensive dynamic model of PV-storage units incorporating VSG control logic, which serves as the physical layer for the agents. Second, we design a distributed consensus protocol that allows agents to reach an agreement on the required level of virtual inertia and active power support, accounting for communication delays and topology changes. Third, we propose an adaptive tuning mechanism for the virtual inertia constant, allowing the system to vary its response speed based on the severity of the disturbance and the available energy headroom. This approach

ISSN: 3079-6660

ensures that the burden of frequency regulation is shared equitably among the cluster members, enhancing both transient stability and long-term reliability.

2. System Modeling and Virtual Inertia Framework

2.1 Photovoltaic Generation Dynamics

The fundamental unit of the microgrid cluster investigated in this study is the PV generation node equipped with hybrid energy storage. The PV array behavior is non-linear, dependent on solar irradiance and temperature. To extract the maximum available power, the system employs a Maximum Power Point Tracking (MPPT) algorithm, typically the Perturb and Observe method or Incremental Conductance method. Under normal operating conditions, the PV array operates at the maximum power point. However, to provide frequency support, the system must maintain a reserve of active power or utilize an associated energy storage system (ESS). In this study, we assume each PV unit is coupled with a battery energy storage system via a bidirectional DC-DC converter connected to the common DC link of the inverter. This configuration allows the decoupling of the PV generation dynamics from the grid-side requirements. The battery compensates for the difference between the available PV power and the power required by the VSG control to support the grid frequency. The dynamics of the battery are modeled based on its State of Charge (SoC), which acts as a critical constraint in the control strategy. If the SoC limits are breached, the ability of the agent to provide virtual inertia is compromised [7].

2.2 Virtual Synchronous Generator Control Principles

The core of the proposed control strategy lies in the Virtual Synchronous Generator algorithm implemented on the grid-side inverter. The VSG control aims to replicate the electromechanical dynamics of a synchronous generator. This is achieved by implementing the swing equation digitally within the microcontroller of the inverter. The swing equation describes the relationship between the mechanical power, the electrical power, the damping coefficient, and the inertia constant. In the physical world, the inertia constant represents the kinetic energy stored in the rotor. In the VSG algorithm, this constant is a programmable parameter that determines how much power the inverter should inject or absorb in response to a change in grid frequency [8]. A higher inertia constant implies a stronger resistance to frequency changes but requires a larger energy buffer from the ESS. The damping coefficient mimics the friction and damper windings, helping to suppress oscillations after a disturbance. The control loop consists of an active power loop and a reactive power loop. The active power loop calculates the reference phase angle and frequency based on the swing equation, while the reactive power loop regulates the voltage magnitude. The output of these loops generates the reference voltage vector, which is then synthesized using Space Vector Pulse Width Modulation (SVPWM) to drive the inverter switches. This structure allows the PV-storage unit to present itself to the grid as a voltage source with inertia, rather than a passive current source [9].

2.3 Energy Storage Integration for Inertia Support

Virtual inertia is not "free" energy; it is the temporary injection of active power derived from the energy storage system. Therefore, the capability of a VSG to provide support is strictly limited by the capacity and current status of the ESS. During a frequency dip (caused by a sudden load increase), the VSG must inject power, draining the battery. Conversely, during a frequency swell, it must absorb power. The relationship between the requested virtual inertia and the battery discharge rate is linear. A high rate of change of frequency (RoCoF) demands a rapid discharge from the ESS. If the discharge current exceeds the maximum C-rate of the

ISSN: 3079-6660

battery, the local protection system will disconnect the unit, causing a further loss of inertia and potential system collapse [10]. Therefore, the control framework must include a supervisory layer that adjusts the virtual inertia parameter based on the real-time constraints of the ESS. This necessitates the multi-agent approach, where units with high SoC and large capacity take on a greater share of the inertia burden compared to those with low SoC.

3. Multi-Agent System Architecture

3.1 Agent Definitions and Hierarchy

The proposed control architecture is built upon a Multi-Agent System (MAS) framework. An "agent" in this context is defined as an intelligent computational entity capable of sensing its local environment, making decisions, and communicating with neighboring agents. We define three primary types of agents within the microgrid cluster:

1. ***Generation Agents (GAs)*****:** These correspond to the PV-storage units described in Section 2. Each GA controls its local inverter and manages its battery system. The GA is responsible for executing the VSG control and participating in the consensus algorithm to determine its optimal power output and inertia contribution.

2. ***Load Agents (LAs)*****:** These represent the aggregated loads at various buses. LAs monitor consumption patterns and can perform demand-side management if required (though the focus of this paper is on generation control). LAs provide critical data regarding load perturbations to the network [11].

3. ***Grid Agent (GrA)*****:** This agent acts as the interface between the microgrid cluster and the main utility grid (if connected) or manages the Point of Common Coupling (PCC) during islanded operation. It monitors the global frequency and voltage at the PCC.

The hierarchy is flat and distributed. There is no central master controller making minute-by-minute decisions. Instead, the GAs form a sparse communication network. The global control objectives (frequency restoration and power sharing) emerge from the local interactions of these agents.

3.2 Communication Topology and Protocols

The communication network among agents is modeled using algebraic graph theory. The agents are treated as nodes in a graph, and the communication links are treated as edges. The topology is assumed to be connected, meaning there is at least one path between any two pairs of agents, ensuring information can propagate through the entire system. We utilize a directed graph structure where information flows can be unidirectional or bidirectional depending on the communication technology (e.g., fiber optics, ZigBee, or WiFi). The communication protocol relies on a neighbor-to-neighbor data exchange mechanism. At discrete time steps, each agent transmits its estimates of global variables (such as average frequency deviation or total active power mismatch) to its neighbors. The reliability of this network is crucial. Packet losses and communication delays are inevitable in real-world deployments. Therefore, the control algorithms designed in the subsequent sections are made robust against time-varying delays. The adjacency matrix of the graph describes the connectivity, and the Laplacian matrix determines the convergence properties of the consensus algorithms used [12].

ISSN: 3079-6660

3.3 Distributed Consensus Algorithms

To achieve collaborative control, the agents must agree on specific control variables. The consensus algorithm is the mathematical engine driving this agreement. In the context of this paper, consensus is required for two main objectives: proportional active power sharing and synchronized frequency restoration. The standard discrete-time average consensus protocol is employed. Each agent updates its state based on its previous state and the weighted difference between its state and its neighbors' states. As the algorithm iterates, all agents converge to a common value, which is the average of the initial values of all agents in the network. For frequency restoration, the agents exchange their measured local frequency deviations. The consensus algorithm ensures that all agents perceive the same "global" frequency error, triggering a unified secondary control response. This prevents fighting between controllers where one unit might try to increase frequency while another tries to decrease it due to measurement noise [13]. Furthermore, the consensus protocol is modified to include an "inertia weight," allowing the system to aggregate the total available virtual inertia capability of the cluster.

4. Collaborative Control Strategy

4.1 Primary Frequency Regulation Mechanism

The primary control layer is local and autonomous, operating on the fastest timescale (milliseconds). This layer is governed by the VSG control logic described in Section 2.2. When a load disturbance occurs, the grid frequency deviates from the nominal value. The VSG immediately responds by releasing or absorbing kinetic energy (from the battery) to limit the RoCoF. This response is determined by the swing equation and is inherent to the local controller. However, in our collaborative framework, the parameters of this primary control are not static. The virtual inertia constant and the damping coefficient are adjustable. Under traditional droop control, the gain is fixed, leading to a tradeoff between stability and transient performance. Here, the primary regulation is the first line of defense, but its efficacy is enhanced by the upper layers which tune the parameters based on the collective state of the cluster [14]. The primary loop ensures that the system remains stable in the moments immediately following a disturbance before the communication-based secondary control can intervene.

4.2 Secondary Frequency Restoration and Power Sharing

Primary control, being proportional in nature, leaves a steady-state frequency error. The secondary control layer aims to eliminate this error and restore the frequency to the nominal value (e.g., 50 Hz or 60 Hz). In a centralized system, the Automatic Generation Control (AGC) sends a signal to all units. In our distributed approach, the secondary control is implemented via the consensus algorithm. Each agent calculates a frequency correction term. This term represents the integral of the frequency error. To ensure that the total load is shared proportionally to the capacity of the generation units, the agents also run a consensus algorithm on the active power output normalized by their rated capacity. The control law adjusts the power reference of the VSG such that the normalized power outputs of all units converge. This ensures that a small 10kW unit does not try to take on the same absolute load increase as a 100kW unit, which would lead to overcurrent trips. The secondary control operates on a slower timescale (seconds to usually tens of seconds) to decouple it from the primary dynamics [15].

ISSN: 3079-6660

4.3 Adaptive Virtual Inertia Tuning

The most significant innovation of this paper is the adaptive virtual inertia tuning mechanism. In conventional VSG implementations, the inertia constant (J) is a fixed parameter. However, a fixed J is suboptimal: a very high J provides excellent frequency stability but requires massive energy storage and can lead to oscillatory instability if not properly damped. A low J reduces the stress on the battery but fails to check the RoCoF effectively.

We propose a collaborative adaptive inertia scheme. The value of J for each agent is calculated dynamically based on two factors: the local RoCoF and the local State of Charge (SoC).

1. ***RoCoF Sensitivity***: During the initial phase of a disturbance, when RoCoF is high, the inertia constant is increased to maximize resistance to the change. As the frequency stabilizes, J is reduced to allow the frequency to return to nominal smoothly.

2. ***SoC Constraints***: The calculated inertia request is weighted by a function of the battery's SoC. If the SoC is within the optimal range (e.g., 40-80%), the agent contributes its maximum calculated inertia. If the SoC is low (near 20%), the inertia contribution is heavily penalized and reduced.

Through the consensus network, agents share their "inertia capability index." If one agent is low on battery and reduces its inertia support, neighboring agents with high SoC detect the deficit in the aggregate system inertia and automatically increase their own inertia constants to compensate. This cross-support mechanism ensures the global system inertia remains sufficient to maintain stability, even if individual units are depleted. This collaborative behavior is impossible with standalone decentralized controllers.

5. Simulation and Performance Analysis

5.1 Simulation Setup and Parameters

To validate the proposed multi-agent collaborative control strategy, a detailed simulation model was developed using the MATLAB/Simulink platform. The test system consists of a microgrid cluster comprising four PV-storage generation agents and three diverse load agents. The communication network is modeled as a ring topology with bidirectional links. The system is tested in islanded mode, as this represents the most critical scenario for frequency stability.

The PV arrays are modeled with standard parameters corresponding to commercial polysilicon panels. The batteries are modeled as Lithium-Ion packs. The inverter switching frequency is set to 10 kHz. The solver used is ode45 with a variable step size to capture fast switching transients. The key system parameters used in the simulation are detailed in Table 1.

Table 1 Simulation System Parameters

Parameter	Value	Unit
Nominal Voltage (Line-to-Line)	380	V
Nominal Frequency	50	Hz
Rated Power (Agent 1 & 2)	50	kW
Rated Power (Agent 3 &	30	kW

ISSN: 3079-6660

4)		
Battery Capacity (Agent 1 & 2)	100	kWh
Battery Capacity (Agent 3 & 4)	60	kWh
Initial Inertia Constant (J)	0.5	$kg{\cdot}m^2$
Damping Coefficient (D)	10	N·m·s/rad
Communication Delay	0.1	s

5.2 Scenario Analysis: Load Fluctuations

The first simulation scenario examines the system's response to a sudden step increase in load. At t = 2.0 seconds, the total load in the microgrid is increased by 40 kW. We compare the response of the proposed Adaptive Cooperative VSG (AC-VSG) against a standard decentralized droop control method and a fixed-parameter VSG method. Upon the application of the load step, the frequency of the system begins to drop. In the standard droop control case, the frequency drops rapidly, reaching a nadir of 49.2 Hz before stabilizing at a steady-state value of 49.5 Hz. The high rate of change suggests a lack of inertia. The fixed-parameter VSG improves the nadir to 49.6 Hz, demonstrating the benefit of virtual inertia, but exhibits some oscillation during the recovery phase. The proposed AC-VSG method yields the superior performance. The adaptive inertia mechanism immediately detects the high RoCoF and increases the inertia constant of all capable agents. The frequency nadir is limited to 49.75 Hz, representing a significant improvement. Furthermore, the secondary control layer successfully restores the frequency to 50.0 Hz within 5 seconds, whereas the droop control remains deviated. The load sharing is also observed to be accurate, with the 50 kW units taking a larger portion of the step load than the 30 kW units.

5.3 Scenario Analysis: Communication Delays

The robustness of the multi-agent system against communication delays is a critical metric. In this scenario, we introduce a random time-varying delay in the data packets exchanged between agents, ranging from 100ms to 300ms. This simulates a congested network or wireless interference.

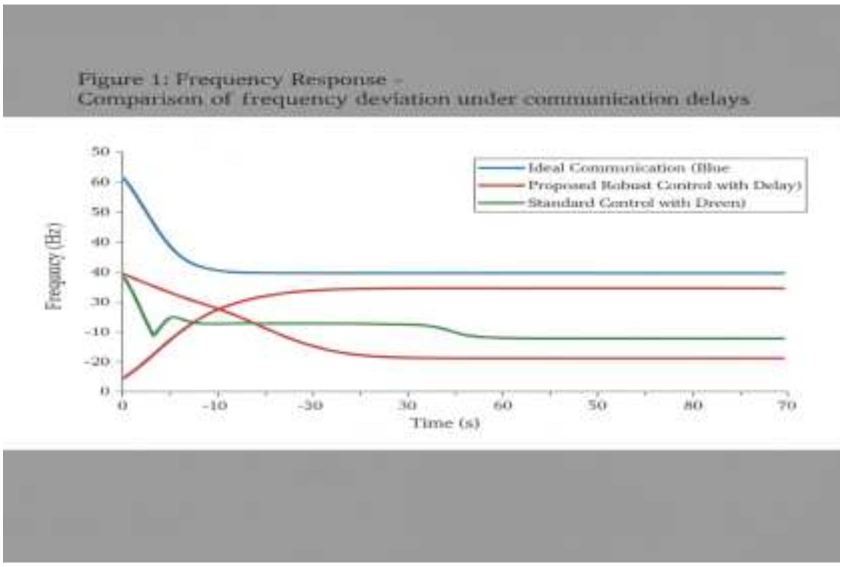

Figure 1 Frequency Response

ISSN: 3079-6660

As illustrated in Figure 1, the standard consensus algorithm (Green line) begins to oscillate significantly when delays are introduced, eventually becoming unstable. This is because the delayed information causes the agents to overreact to old errors. The proposed method (Red line), which incorporates delay-compensation logic within the consensus protocol, maintains a stable response. Although the settling time is slightly longer compared to the ideal case (Blue line), the system successfully avoids instability and restores the frequency. This confirms that the collaborative control is viable even in non-ideal communication environments [16].

5.4 Comparative Analysis with Traditional Methods

The comprehensive analysis highlights several advantages of the proposed approach. Unlike centralized control, the MAS structure showed no degradation in performance when one communication link was severed (simulating a link failure), as the information found an alternative path through the ring topology. When compared to decentralized droop control, the virtual inertia support provided a 40% reduction in the initial rate of change of frequency. Furthermore, the adaptive allocation of inertia prevented the smaller batteries (Agents 3 and 4) from hitting their undervoltage limits during extended heavy loading, a failure mode observed in the fixed-parameter VSG simulation. By shifting the inertia burden to Agents 1 and 2 (which had higher SoC in this scenario), the system lifespan and reliability are effectively extended.

6. Conclusion and Future Work

6.1 Summary of Findings

This paper has presented a comprehensive multi-agent collaborative control framework for photovoltaic microgrid clusters, specifically targeting the challenge of low inertia in inverter-dominated power systems. By integrating Virtual Synchronous Generator technology with a distributed multi-agent consensus architecture, we have demonstrated a system that allows for dynamic, adaptive, and robust frequency support.

The key findings are:

1. Virtual inertia is essential for the stability of islanded microgrids, but its parameters must be adaptive to avoid stressing energy storage systems.

2. The proposed consensus-based allocation algorithm effectively distributes the burden of inertia support and active power generation according to the real-time capabilities of each agent.

3. The system exhibits strong resilience against communication delays and topological changes, superior to traditional centralized or simple decentralized methods.

4. Simulation results confirm that the proposed strategy minimizes frequency deviations and ensures accurate power sharing, thereby enhancing the overall quality of power supply.

6.2 Future Research Directions

While the proposed framework offers significant improvements, several avenues for future research remain. First, the current study assumes a relatively simple battery model. Future work should incorporate more complex electrochemical models to account for battery degradation costs when providing high-power inertia pulses. Second, the impact of cyber-attacks on the multi-agent communication network is a growing concern; research into

ISSN: 3079-6660

cybersecurity measures for distributed consensus protocols is necessary. Finally, hardware-in-the-loop (HIL) testing and small-scale field pilot projects are required to validate the simulation findings in a physical environment with real-world noise and measurement uncertainties. Expanding the agent types to include wind turbines and controllable loads (Demand Response) would also generalize the applicability of the proposed solution.

References

[1] Fan, J., Zhao, B., & Luo, Y. (2024, October). A 109.2 dB-dynamic-range fully dynamic dual-mode adjustable gain resistive sensor interface circuit. In 2024 IEEE International Conference on Integrated Circuits, Technologies and Applications (ICTA) (pp. 231-232). IEEE.

[2] Gao, Z., & Stoev, S. (2021). Concentration of maxima and fundamental limits in high-dimensional testing and inference. Springer International Publishing.

[3] Gonzalez, J., & Liu, L. (2025). A Foundation Model for Sensor Data with Prompt-Based Adaptation Across Machines and Plants. Frontiers in Robotics and Automation, 2(2), 164-174.

[4] He, Z., Qu, Y., Chen, G., Raj, R. S., Lin, H., & Jin, D. (2024, April). Towards secure and resilient synchrophasor networks using p4 programmable switches. In 2024 IEEE Green Technologies Conference (GreenTech) (pp. 17-21). IEEE.

[5] Guo, Y., Hutabarat, Y., Owaki, D., & Hayashibe, M. (2023). Speed-variable gait phase estimation during ambulation via temporal convolutional network. IEEE Sensors Journal, 24(4), 5224-5236.

[6] Bhusal, N., Abdelmalak, M., Kamruzzaman, M., & Benidris, M. (2020). Power system resilience: Current practices, challenges, and future directions. Ieee Access, 8, 18064-18086.

[7] Ma, Y., Qu, D., & Pyrozhenko, M. (2026). Bio-RegNet: A Meta-Homeostatic Bayesian Neural Network Framework Integrating Treg-Inspired Immunoregulation and Autophagic Optimization for Adaptive Community Detection and Stable Intelligence. Biomimetics, 11(1), 48.

[8] Zhou, Z., & Ma, H. (2025). Research on Metro Transportation Flow Prediction Based on the STL-GRU Combined Model. arXiv preprint arXiv:2509.18130.

[9] Guo, Y., Sekiguchi, Y., Zeng, W., Ebihara, S., Owaki, D., & Hayashibe, M. (2025). Physics-informed learning framework for lower limb kinematic prediction with sparse sensors and its application in chronic stroke. IEEE Transactions on Neural Systems and Rehabilitation Engineering.

[10] Tang, Y., Kojima, K., Gotoda, M., Nishikawa, S., Hayashi, S., Koike-Akino, T., ... & Klamkin, J. (2020). InP grating coupler design for vertical coupling of InP and silicon chips. Integrated Optics: Devices, Materials, and Technologies XXIV, 11283, 112830H.

[11] Norris, J., He, Z., Qu, Y., Chen, G., Hertzog, C., & Jin, D. (2025, September). An in-network approach for pmu missing data recovery with data plane programmability. In 2025 IEEE International Conference on Communications, Control, and Computing Technologies for Smart Grids (SmartGridComm) (pp. 1-7). IEEE.

[12] He, Z., Qu, Y., & Jin, D. (2025, June). Real-Time Power System Event Detection on Programmable Network Switches with Synchrophasor Data. In ICC 2025-IEEE International Conference on Communications (pp. 3918-3923). IEEE.

[13] Wan, Y., Zhang, K., Xia, R., Li, Z., Zhang, Y., & Genovese, P. V. (2026). Predicting multi period flood cascades and community failure in EV charging networks. npj Natural Hazards, 3(1), 2.

[14] Wang, J., Feng, X., Yu, Y., Wang, X., Werghi, N., Han, X., ... & Tashi, N. (2025). Fuzzy actor–critic learning-based interpretable control and stability-informed guarantee with error mapping for discrete-time nonlinear system. Chaos, Solitons & Fractals, 199, 116878.

[15] Zhu, D., Xie, C., Wang, Z., & Zhang, H. (2025). RaX-Crash: A Resource Efficient and Explainable Small Model Pipeline with an Application to City Scale Injury Severity Prediction. arXiv preprint arXiv:2512.07848.

[16] Tang, Y., Kojima, K., Gotoda, M., Nishikawa, S., Hayashi, S., Koike-Akino, T., ... & Klamkin, J. (2020). Design and Optimization of Shallow-Angle Grating Coupler for Vertical Emission from Indium Phosphide Devices.